Textile Research Journal

Original article

Mitigation of firefighters' skin burn injuries utilizing auxiliary measures

Textile Research Journal
0(0) 1–14

DOI: 10.1177/00405175221147245
journals.sagepub.com/home/trj
SAGE

Rumeel A Bhutta and Sengkwan Choi

Abstract

The improvement in the thermal resistance of firefighter's outer garments has been traditionally achieved with the implementation of phase change materials or aerogel as an added protective measure. This study proposes supplementary novel cost-effective measures to enhance the thermal resistance of conventional firefighter outer garments. The proposed measures consist of auxiliary protective layers of meta-aramid fabric of a plain weave and a honeycomb structure. A custom built vertically oriented bench-scale apparatus was used to simulate extreme to life-threatening fire environments characterized in terms of an incident radiative flux of 84 kW/m^2 and 126 kW/m^2. The fluctuations in experimental heat flux density were treated by employing a Gaussian empirical model. The heat dissipation rate within the skin layers was predicted with a numerical model based on finite element methodology. The skin burns were classified with Henrique's integral. The conventional outer garment when exposed to 84 kW/m^2 and 126 kW/m^2 resulted in a superficial second and third-degree burn. The auxiliary layers, in conjunction with the outer garment, mitigated second and third-degree burns. The meta-aramid fabric of a plain weave exhibited better thermal resistance than the honeycomb structure layer. The proposed measures reduced the epidermis temperature by 32%. An inner garment made of meta-aramid fabric is recommended to be worn concurrently with an outer protective suit for severe fire incidents due to its relative ease of use. Honeycomb structure layers are not recommended due to their weak structure and restriction in mobility.

Keywords

High performance fabrics, fire resistance fabrics, measurements, performance, protective and other high-performance clothing systems, properties

Thermal protective clothing is of great importance in firefighting due to the high probability and unpredictability of fire accidents in a compartment setting or a forest fire.[1] This suit can be categorized as: (a) station wear – single layer garment worn in the fire station; and (b) turnout gear – multiple layer garment worn when reporting to fire incident.[2] A turnout gear consists of three fabric layers: (a) an outer shell (OS); (b) a moisture barrier (MB); and (c) a thermal liner (TL). It is designed to shield from various fire conditions, categorized as routine, hazardous and emergency.[3,4] The work in this study focuses on the implementation of the turnout gear and proposes measures to improve its performance in severe thermal environments.

The performance of turnout gear has been majorly associated with thermophysical characteristics of aramid fabrics.[5–9] However, recent studies have shown that orientation also influences the assessment of these fabrics, and concluded that horizontal configuration underestimates performance level,[10] with a similar finding on cone calorimeter orientation tests.[11] A vertical orientation, in bench-scale testing, depicts the actual body position.[12–14] Therefore, it is preferred over horizontal configuration. A standard value of incident heat flux of 84 kW/m^2, proposed by Behnke in 1984,[15] is accepted as an upper limit for flash fire.

Belfast School of Architecture and the Built Environment, Ulster University, Northern Ireland, UK

Corresponding author:
Sengkwan Choi, Belfast School of Architecture and the Built Environment, Ulster University, 2-24 York Street, Belfast BT15 1AP, UK.
Email: sengkwanchoi@hotmail.com

International test standards such as NFPA 1971[16] and ISO 6942:2002[17] have adopted 84 kW/m^2 as a representation of emergency conditions. Experiments conducted on modern compartment settings have been shown to exceed this limit and can reach 150 kW/m^2.[18,19] To date, no performance data are available in the literature for heat flux greater than 84 kW/m^2, to the best knowledge of the authors. This study addresses this by accessing a turnout gear in a vertical orientation subjected to an incident heat flux of 84 and 126 kW/m^2, a representation of emergency/extreme and life-threatening conditions.

Researchers have proposed several approaches to reduce skin burn injuries by employing different techniques. The increase in fabric thickness and air gap enhances fabric performance.[20–22] The application of shape memory alloy, which at a certain actuation temperature expands the cavity between fabric layers, enhances insulation capability.[23] Thermal conductivity and specific heat had a significant effect on fabric performance relative to optical properties such as emissivity, transmissivity and reflectivity.[24] Controlling radiative heat transfer with the application of the aluminum coating on the fabric takes advantage of the reflective property of aluminum.[25] However, it is recommended only for radiant exposure, as on flame contact aluminum coating degrades.[26] This concept has also recently been investigated for nano silver coating on the external surface of the fabric assemble, for 10–20 kW/m^2 of incident radiative flux, with prominent improvement reported compared with uncoated fabric.[27] These studies addressed a novel aspect of improving fabric performance which is either physically impossible to implement with existing protective assemble or requires rigorous manufacturing. Moreover, air gaps between fabric layers cannot be controlled and will vary with the position on the body.[28,29] A more practical approach to improving the performance of the existing garment is the use of aerogel or TLs treated with aerogel, which can enhance existing assemble performance by approximately 10%, with a reduction of weight by 24.3%.[30,31] To improve the performance of the protective garment, its capacity to store thermal energy must be improved. Phase change materials (PCMs) that absorb latent heat by altering their phase from solid to liquid or vice versa have been proposed.[32,33] An improvement in performance was documented when PCM was positioned adjacent to the innermost layer[34] or close to the skin for the incident flux of 84 kW/m^2.[35] The increase in thickness was found to be directly related to the improved performance.[36]

Most PCMs are flammable and their application in firefighting clothing, near a fire, is not recommended. To this end, a combination of organic PCMs with aerogel treated TL reported better performance output, to delay burn injuries as opposed to using either of them separately.[37] Treating the TL or any fabric layer of the turnout gear increases its overall weight. A recent study conducted by placing an underlayer to an existing multilayered suit to predict thermal comfort showed a positive relationship; however, little information was provided on thermal protection.[38] A TL cut into the honeycomb structure using laser replacing conventional TL structure was implemented and tested for an incident flux of 83 kW/m^2 in a horizontal orientation.[39]

The existing literature on improving thermal performance requires a rigorous approach to be embedded into an existing turnout gear. The application of underlayer and honeycomb, as auxiliary measures, is promising and is further explored in this study. Implementing it requires minimum adjustment to the existing turnout gear. It can be exercised when severe fire conditions are expected. Radiative flux is selected in accordance with the ISO 6942 standard recommendation for vertical orientation to depict a standing individual. It will help in mitigating firefighter fatalities by providing increased performance and delaying burn injuries.

Test apparatus

The test apparatus utilized for this study is shown in Figure 1, developed by the cooperation of Korean Conformity Laboratories (KCLs) and Ulster University. It consists of a radiant panel, a specimen assembly shown

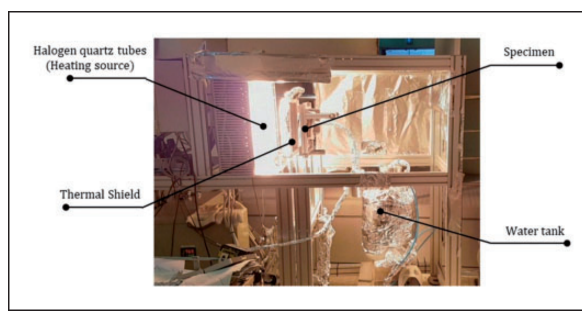

Figure 1. Test apparatus.

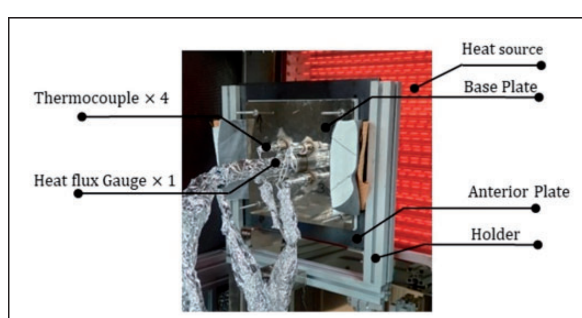

Figure 2. Experimental set-up.

in Figure 2, and a trolley. The two-layered halogen quartz tube can output a consistent radiant flux of 126 kW/m^2 for more than 60 s. To keep radiant panels from overheating a water channel was used. The apparatus specimen has an assembly of 200 cm × 200 cm, that can grip multiple fabric layers with a 2 N force. A 100 cm × 100 cm fabric area of the test sample can be exposed to radiative heat flux. Four type K thermocouples were attached to the back of the fabric using pressure contact to record the temperature of the innermost layer. Irradiance at skin surface level was logged using a heat flux gauge. The test apparatus was configured in a vertical orientation. The apparatus consistency and development procedure have been detailed and discussed in the KCL publication.[40]

Specimen preparation

In Figure 3(a) a conventional lay-up of the turnout gear is presented consisting of fabric layers such as:

- OS: to resist heat, protect the wearer from chemical spills, blood and flames and alternatively, let pass vapors from body sweat.
- MB: an added aid in heat resistance and control of moisture flow.
- TL: for comfort, to provide additional heat resistance and permit metabolic heat release to the environment.

A 2 mm air spacing was ensured between the fabric layers and 6.5 mm between the TL and the substrate. These spacings are representative of average airgaps reported based on three-dimensional (3D) scanning.[28,41–43] In addition to the lay-up shown in Figure 3 (a), two more lay-ups were prepared according to Figure 3(b) and (c). In Figure 3(b) an additional layer of Nomex underwear,[44] worn by formula 1 drivers, was inserted at a distance of 5 mm from TL and 2 mm behind the substrate. In Figure 3(c) a Nomex honeycomb[45] structure layer replaces the air gap between the MB and TL. Type A, selected as benchmark, is a currently adopted protective assemble in the Korean Fire Service. Types B and C are enhancements of type A with additional layers, based on availability for practical applications. The specimens were preconditioned at room temperature and relative humidity of 65%.[16] Physical characteristics are summarized in Table 1.

Skin numerical model

Skin tissue damage can be associated with an increase in tissue cells temperature at a certain depth.[46–49]

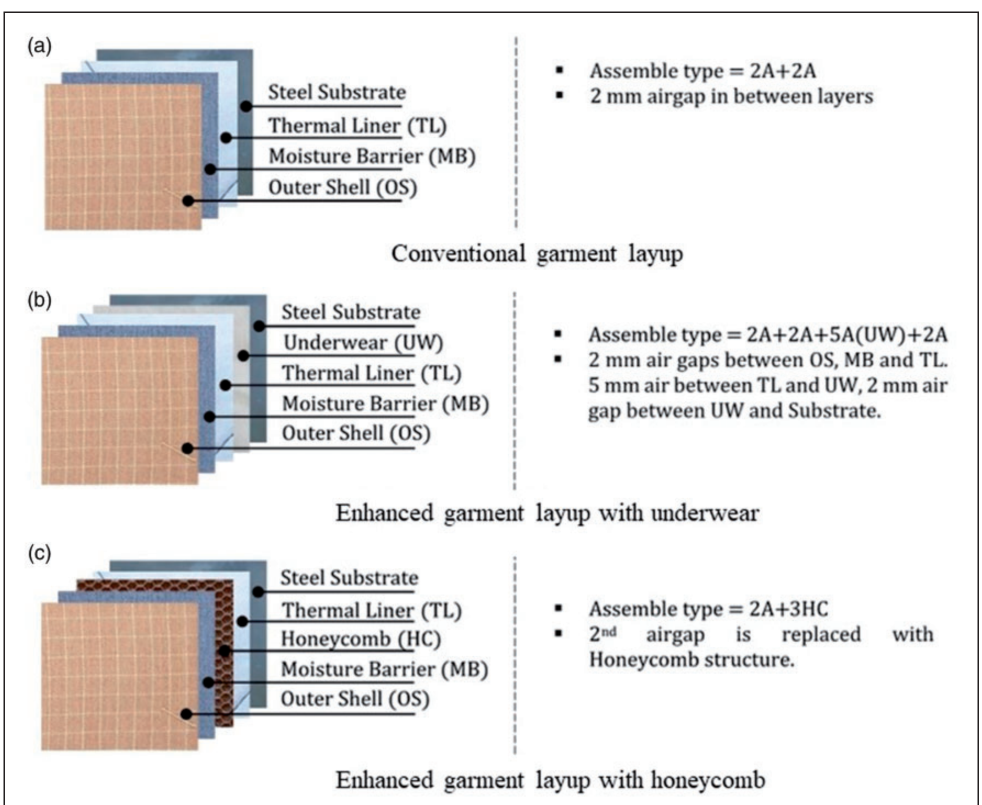

Figure 3. Three protective assembly lay-ups: types A, B, and C. (a) Conventional garment layup; (b) enhanced garment layup with underwear and (c) enhanced garment layup with honeycomb.

Table 1. Specimen physical characteristics

Outer shell (OS)	Material: Aramid fabric 100% (meta aramid 80%, papa-aramid 20%)	
	Weight: 209 g/m^2	Pattern: Ripstop
	Thickness: 0.40 mm	
Moisture barrier (MB) (Substrate + PTFE film)	Material: Meta-aramid 100% (Substrate) + PTFE film	
	Weight: 190 g/m^2	Pattern: Plain weave
	Thickness: 0.347	
Felt insulation of thermal liner (TL)	Material: Meta aramid 100%	
	Weight: 149 g/m^2	Applied layer: Quilt with an inner layer
Face cloth of thermal liner (TL)	Material: Meta aramid 100% (face cloth)	
	Weight: 149 g/m^2	Pattern: Plain weave
	Thickness: 1.754	
Underwear (UW)	Material: Meta aramid 100%	
	Weight: –	
	Thickness: 0.61 mm	
Honeycomb (HC)	Material: Meta aramid 100%	
	Weight: –	
	Thickness: 3 mm	

A bio-heat transfer model proposed by Pennes[50] is used for finite element (FE) analysis, as shown in equation (1). It is based on the Fourier law of heat conduction with heat exchange between tissue and blood with metabolic heat generation. The numerical model is developed based on FE methodology solved on a commercially available package ABAQUS®Standard. The transmitted irradiance recorded by the apparatus is implemented as an initial boundary condition to predict skin temperatures:

$$\rho C_p \frac{\partial \theta}{\partial t} = \frac{\partial}{\partial x}\left(k \frac{\partial \theta}{\partial x}\right) + \omega_b (\rho C_p)|_b (\theta_a - \theta) + \mathrm{Q}_m \quad (1)$$

where

ω_b Is the blood perfusion rate, kg/m^3 s

$(\rho C_p)|_b$ Is the volumetric heat capacity (blood), J/m^3.°C

T$_a$ Is the arterial temperature/core body

Q$_m$ Is the metabolic heat generation/tissue heat generation rate, W/M^3.

Rigorous testing of equation (1) has shown that the profusion term, $[(\rho C_p)|_b(\theta_a - \theta)]$, had no impact on the thermal conductivity of skin under short exposure duration.[51] Correlating it with a study of Lipkin and Hardy,[52] it takes at least 20 s for the skin to react to external stimuli (heat flux), by increasing blood flow. The skin emissivity of 0.94 has a negligible effect on skin temperature; that is, radiant exchange from the skin to the environment.[49] Moisture evaporation and carbonization of the skin occurs after second and third-degree burns. These assumptions are applied in this study, for the condition at 84 and 126 kW/m^2. Hence, equation (1) is solved in variational form[53] with the afore-mentioned assumptions as:

$$\iiint_V \delta\theta\rho\dot{\mathrm{U}}\mathrm{dV} - \iiint_V \frac{\partial \theta}{\partial x} . q\mathrm{dV} = \iint_S \delta\theta q \mathrm{dS} + \iiint_V \delta\theta \mathrm{Q} \mathrm{dV} \quad (2)$$

where $\delta\theta$ is an arbitrary variational field satisfying the essential boundary conditions, ρ is the density of the fabric, $\dot{\mathrm{U}}$ is the fabric time rate of the internal energy, q is the heat flux, V is the volume. The variation method of thermal energy balance is applied as the basis of discretization in the FE model on the four-node linear quadratic element. Time integration is performed utilizing a modified form of the crack–Nicolson method,[54] as in equation (3):

$$\dot{U}_{t+\Delta t} = \frac{U_{t+\Delta t} - U_t}{\Delta t} \quad (3)$$

The accuracy of the numerical model is verified against:

(1) Stoll and Greene experimental data.[49]
(2) FE model of skin developed by Torvi and Dale using Galerkin's weighted residual method.[51]
(3) Closed-form solution by Griffith and Hortan for two-layered material using Laplace transform with correction,[55,56] subject to boundary conditions as:

$$f\ (x, t) = \theta(x, t) - \theta(x, 0)$$

$$\frac{\partial f_1}{\partial t} = \alpha_1 \frac{\partial^2 f_1}{\partial x^2},\ \ 0 \leq x \leq x_\aleph$$

$$\frac{\partial f_2}{\partial t} = \alpha_2 \frac{\partial^2 f_2}{\partial x^2}, \quad x_{\aleph} \le x$$

$$-k_1 \frac{\partial f_1}{\partial x} = q \text{ for } t \ge 0 \tag{4}$$

For layer 1:

$$f_1(x,t) = \frac{q}{k_1}\left[\left\{2\sqrt{\frac{\alpha_1 t}{\pi}} e^{\left(\frac{-x^2}{4\alpha_1 t}\right)} - x erfc\left(\frac{x}{\sqrt{4\alpha_1 t}}\right)\right\}\right.$$
$$- \frac{1}{\gamma}\sum_{n=0}^{\infty}\left(-\frac{1}{\gamma}\right)^2 \left\{\left(2\sqrt{\frac{\alpha_1 t}{\pi}}\left(e^{-\left(\frac{x+2L_1(n+1)^2}{4\alpha_1 t}\right)}\right.\right.\right.$$
$$+e^{-\left(x-2L_1(n+1)^2/_{4\alpha_1 t}\right)}))$$
$$-(x+2L_1(n+1)) erfc\left(\frac{x+2L_1(n+1)}{\sqrt{4\alpha_1 t}}\right)$$
$$\left.\left. +(x+2L_1(n+1)) erfc\left(\frac{x+2L_1(n+1)}{\sqrt{4\alpha_1 t}}\right)\right\}\right] \tag{5}$$

For layer 2:

$$f_2(x,t) = \frac{2q\lambda\sqrt{\alpha_1}}{\gamma}\left[\sum_{n=0}^{\infty}\left(-\frac{1}{\gamma}\right)^2\right.$$
$$\left[2\sqrt{\frac{\alpha_1 t}{\pi}}\left(\exp\left(\frac{-\left(x-L_1\left(1-\sqrt{^{\alpha_2}/_{\alpha_1}}(2n+1)\right)\right)^2}{4\alpha_2 t}\right)\right)\right.$$
$$-\left(x-L_1\left(1-\sqrt{^{\alpha_2}/_{\alpha_1}}(2n+1)\right)\right)$$
$$\left.\left. erfc\left(\frac{x-L_1\left(1-\sqrt{^{\alpha_2}/_{\alpha_1}}(2n+1)\right)}{\sqrt{4\alpha_2 t}}\right)\right]\right]$$

For basal layer temperature, $x = x_{\aleph}$ equation (5) becomes:

$$f_b(x,t) = \frac{q}{k_1}\left[\sum_{n=0}^{\infty}\left(-\frac{1}{\gamma}\right)^n\left(1-\frac{1}{\gamma}\right)\left\{2\sqrt{\frac{\alpha_1 t}{\pi}} e^{-\left(\alpha^2\frac{(2n+1)}{\sqrt{4t\alpha_1}}\right)^2}\right.\right.$$
$$\left.\left. -\alpha(2n+1) erfc\left(\frac{\alpha(2n+1)}{\sqrt{4\alpha_1 t}}\right)\right\}\right]$$

where

$$\gamma = \frac{k_2\rho_2 c_{p2} + \sqrt{(kpc_p)_1 (kpc_p)_2}}{k_2\rho_2 c_{p2} - \sqrt{(kpc_p)_1 (kpc_p)_2}},$$
$$\lambda = \left(k_2\sqrt{\alpha_1} - k_1\sqrt{\alpha_2}\right)^{-1}$$

Time temperature histories in the basal layer are plotted in Figure 4, for an irradiance of 4.186 kW/m^2 at nude skin, as recommended by Stoll and Greene.[49] The skin thermal properties are stated in Table 2. Two distinct phases are visible: (a) heating phase of 34 s; and (b) subsequent cooling phase. Predictions made by the variational method closely match the experimental temperature reported by Stoll and Greene in the later part of the exposure. A small deviation is observed at the initial stage of the heating phase with slight over-predictions. Comparing it with Glerkan's weighted residual method,[51] both schemes of FE model predict well for the duration of exposure; however, the variational method predicted better in the cooling phase.

As shown in Figure 5, further verification is conducted at an incident flux of 41 kW/m^2. The results

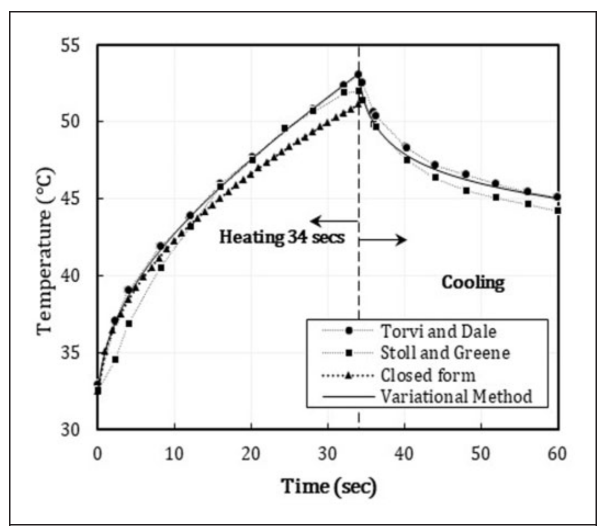

Figure 4. Basel layer temperature history predicted by finite element model and as reported in the literature using numerical analysis and experiments at 4.186 kW/m^2 for 34 s.

Table 2. Skin thermal characteristics[6]

Layer	Thermal conductivity (W/m^2.°C)	Specific heat (J/kg.°C)	Density (kg/m^3)	Thickness (m)
Epidermis	0.255	3598	1200	8×10^{-5}
Dermis	0.253	3222	1200	2×10^{-3}
Subcutaneous	0.167	3760	1000	1×10^{-2}

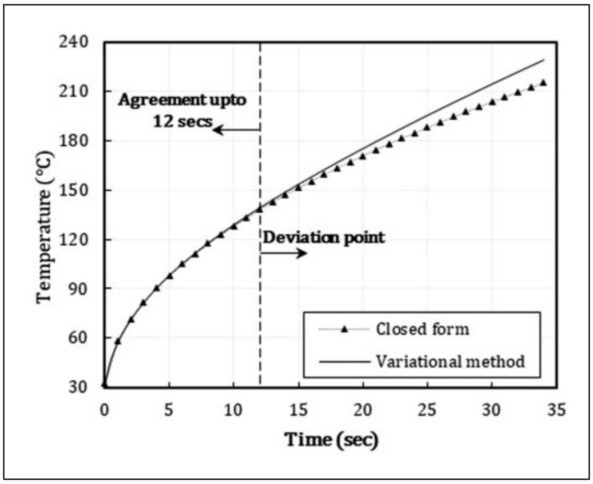

Figure 5. Basel layer temperature history at irradiance of 41 kW/m² for 34 s on nude skin.

are compared to the closed-form solution of the two-layered wall,[55,56] demonstrating agreement up to 12 s, afterwards, deviation occurs. This alteration is associated with limitations in the closed-form solution by Griffith and Hortan, which treats the second layer as semi-infinite with a constant initial temperature of 32°C in the whole domain. This conception introduces no errors in the analytical solution.[55] Whereas, the FE model is three-layered, with a linear temperature gradient applied across the domain from 32°C to 37°C. Hence it is proven that the skin FE model employed in this study can accurately predict skin temperatures.

Henrique integral

Burn damage to the skin is described by Henrique as a chemical rate process of the first order.[46] Skin tissues sustain irreversible damage when the basal layer temperature exceeds the threshold level of 44°C.[46–49] Henceforth, time to superficial (first-degree) or partial thickness burn (second-degree) is approximated by using the basal layer temperature history, for the duration when it is above 44°C, in equation (6). The resulting value of dimensionless integral Ω determines the severity of the skin burn. The values of physical constant for the second-degree were determined by Weaver and Stoll[57] and that of the third-degree burn for the interface between the dermal and subcutaneous layer by Takata as reported by Song et al.[1] Table 3 details the values of these constants and the respective type of burn.

$$\Omega = \int_0^t \mathrm{P}\exp\left(-\frac{\Delta \mathrm{E}}{\mathrm{RT}}\right)\mathrm{d}t \quad (6)$$

Table 3. Henrique physical constants

Constant	Basel layer	Dermal base	Limit
Ω	$\leq$0.50, no burn =0.53, first-degree $\cong$1.00, second-degree	$\cong$1, third-degree	–
P (1/s)	2.185×10^{124} 1.823×10^{51}	4.32×10^{64} 9.39×10^{104}	$44 \leq T \leq 50$°C $T \geq 50$°C
$\frac{\Delta E}{R}$(K)	93,534.9 39,109.8	50,000 80,000	$44 \leq T \leq 50$°C $T \geq 50$°C

where

Ω is the Henriques integral, second-degree burn occurs when Ω is unity.

ΔE is the activation energy (J/mol).

P is the pre-exponential factor.

T is the time-dependent absolute temperature of the basal layer.

Experimental study

Three types of fabric lay-up configuration, types A, B and C, were tested at exposure level of 84 and 126 kW/m², representative of flashover and conditions beyond flashover. Lay-ups were exposed to incident radiant flux for three different durations, detailed in Table 4. Type A lay-up was conventional, as illustrated in Figure 3(a). This type of lay-up is commercially available on the market; therefore, is treated as a benchmark for comparative study of performance with types B and C.

Treatment of experimental data

Type A lay-up was first exposed to an incident flux of 84 kW/m². The heat flux sensor response at the skin level was recorded for exposure durations of 10, 20 and 30 s until the signal drops to zero or negative. It is observed that heat flux obtained from the experiment exhibits a noisy response, as evident from Figure 6. ISO 13506-1 suggests that any negative heat flux recorded by the sensor should be assigned a value of 0 kW/m²; afterwards, a fitting function can be applied to convert it into a steady response.[58] Hence, a Gaussian model[59] is employed as a numerical fitting function in accordance with equation (7):

$$y_{[q]} = \sum_{i=0}^{n} a_i e^{\left[-\left(\frac{x_{[t]}-b_i}{c_i}\right)^2\right]};\ 1 \leq n \leq 8 \quad (7)$$

where $y_{[q]}$ is the adjusted flux response, a is the amplitude, e is the exponential function, b is the centroid, c is the peak width and n is the number of peak widths.

Table 4. Experimental scheme at variable thermal conditions

Exposure (kW/m^2)	Duration	Protective assembly
84 ± 2	10 s	2A + 2A (type A)
	20 s	2A + 2A (type A)
	25 s	2A + 2A (type A)
		2A + 3HC (ttType C)
		2A + 2A + 5A(UW) + 2A (type B)
126 ± 2	10 s	2A + 2A (type A)
	15 s	2A + 2A (type A)
		2A + 3H (type C)
		2A + 2A + 5A(UW) + 2A (type B)
	20 s	2A + 2A (type A)
		2A + 3HC (type C)
		2A + 2A + 5A(UW) + 2A (type B)

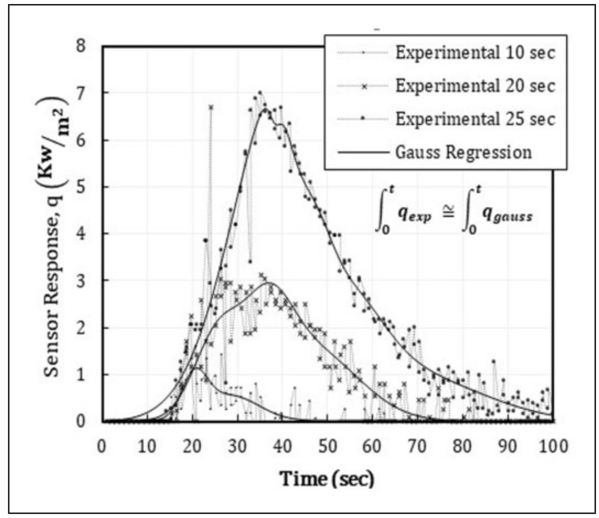

Figure 6. Gaussian model regression fit for type A lay-up at incident flux of 84 kW/m^2.

The steady response is compared with the experimental data, as shown in Figure 6. Gaussian numerical fitting is validated with a trapezoidal numerical integration. The total heat flux received at the skin level estimated with fitting function is in $\geq$90% confidence bounds. This treatment of experimental data is repeated to obtain the irradiance curves for types B and C lay-ups. The converted curves are then applied as a boundary condition for the skin numerical model.

Experimental results

Irreversible skin damage occurs when the basal layer temperature exceeds 44°C.[46–49] This defined criterion is implemented to establish exposure times starting from an initial guess of 10 s. The performance of specimens is evaluated based on transmitted flux, recorded by a heat flux gauge mounted in the substrate. Type A lay-up was first exposed to the incident flux of 84 kW/m^2 and 126 kW/m^2 for 10 s. If the predicted temperature at the basal layer was above 44°C, indicating skin burn, then type B and type C lay-ups were exposed to similar conditions. Otherwise, the exposure time was increased, and the experiment was conducted again for type A. This repeated task was performed until basal layer temperature of 44°C was achieved. Evaluation criteria for the tests is burn degree. Fabrics' thermal degradation and decomposition was ignored.

The performance of each lay-up at an incident flux of 84 kW/m^2 is presented in Figure 7. Peak irradiance observed at the skin level for type A lay-up is $\approx$6.8 kW/m^2. When an additional layer of Nomex underwear (type B) is added, the protection level is improved by $\approx$55% (reduction in transmitted heat flux). When a Nomex honeycomb structure (type C) is inserted, the protection level is improved by $\approx$42%. It is evident that type B and type C performed better than type A under an exposure time of 25 s, with type B performing better than type C. Performance of type B and type C under 10 and 20 s of exposure time is not plotted to keep clarity in the graph; however, it is evident from the 25 s exposure curve that types B and C will perform better under 10 and 20 s exposure duration. A small drop in the maximum irradiance for the type C structure is believed to be associated with the shrinkage of the honeycomb structure layer as observed in the experiments. A small portion of this absorbed energy is then released again, observed as an increase after the drop.

Time temperature histories for the basal and dermal layer are presented in Figure 8. Basel layer temperature for type A at 10 and 20 s exposure remains below the threshold value of 44°C. At an exposure duration of 25 s, this threshold no longer holds, and the skin temperature reaches approximately 55°C. For type B, the skin temperature remains below the threshold value of approximately 42°C. In the case of type C, it reaches $\approx$48°C. Based on these results, the three configurations tested can be ranked as: type B is the best to perform under extreme conditions, followed by type C and then type A. Similar trends are also observed in the predicted temperature distributions at the dermal layer of skin, Figure 8 (right graph).

The performance of types A, B and C protective assembly is also assessed at an upper limit of 126 kW/m^2 to simulate life-threatening fire conditions. Type A lay-up is exposed to an incident flux of 126 kW/m^2 for 10, 15 and 20 s. Type B and C lay-up is exposed under similar incident flux for 15 and 20 s. In Figure 9, the irradiance at skin level under different exposure times is presented. Peak transmitted thermal energy for type A when exposed, for 10 s, is $\approx$2.5kW/m^2; for 15 s, it is $\approx$5kW/m^2 and for 20 s, it

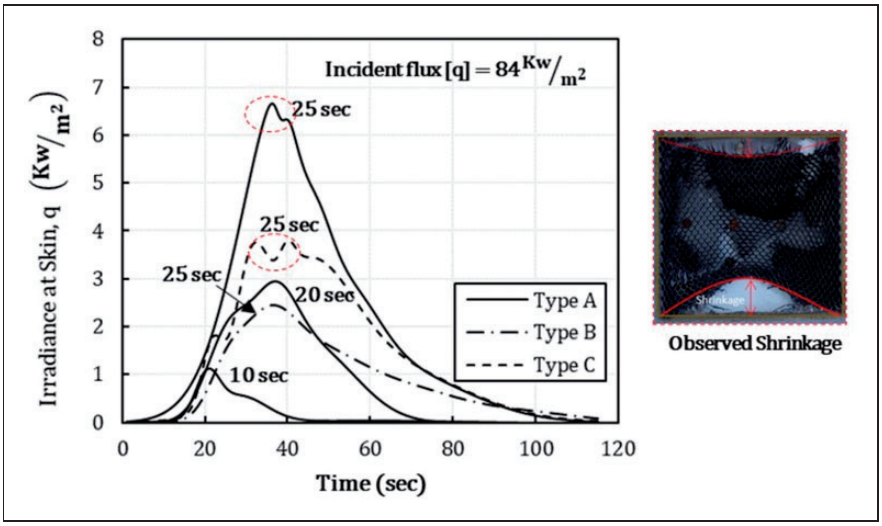

Figure 7. Fabric assemble performance at 84 kW/m^2 and observed shrinkage.

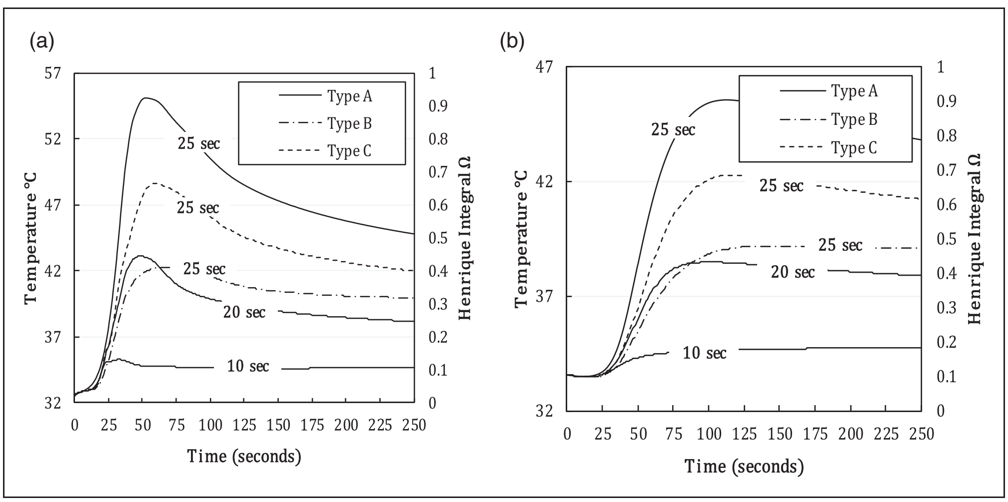

Figure 8. Predicted skin layer temperature at an incident flux of 84 kW/m^2. (a) Basel layer and (b) dermal base.

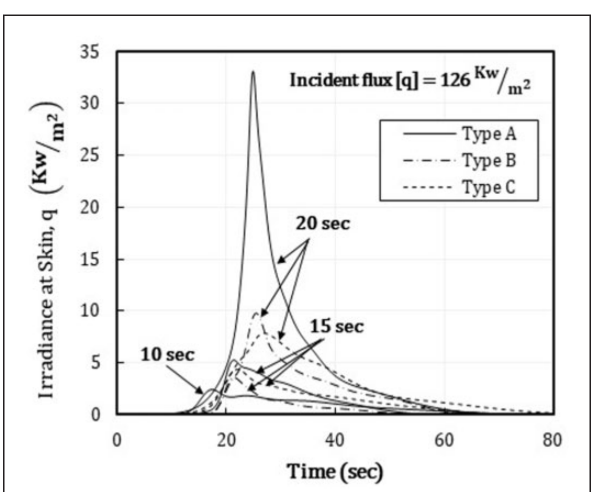

Figure 9. Fabric assemble performance at 126 kW/m^2.

is $\approx$30 kW/m^2, representing failure. This failure is associated with a tear in the OS responsible for direct radiant heat transfer. Type B performed better than type A by limiting irradiance at skin level to $\approx$10 kW/m^2, an improvement of 32% (reduction in transmitted heat flux) for 20 s of exposure time. Type C performed better than type A and type B under 20 s of exposure with an irradiance of $\approx$7 kW/m^2. At 15 s of exposure, types A, B and C all performed close to each other.

The addition of an extra layer (types B and C) proved to be beneficial for working under life-threatening conditions. The added underlayer improved protection from burn injuries by 32%. The temperature time history of types A, B and C is presented in Figure 10 for an incident flux of 126 kW/m^2. Type A lay-up performed well for exposure time up to 15 s. When the exposure duration is more than 15 s, type A failed. At the basal

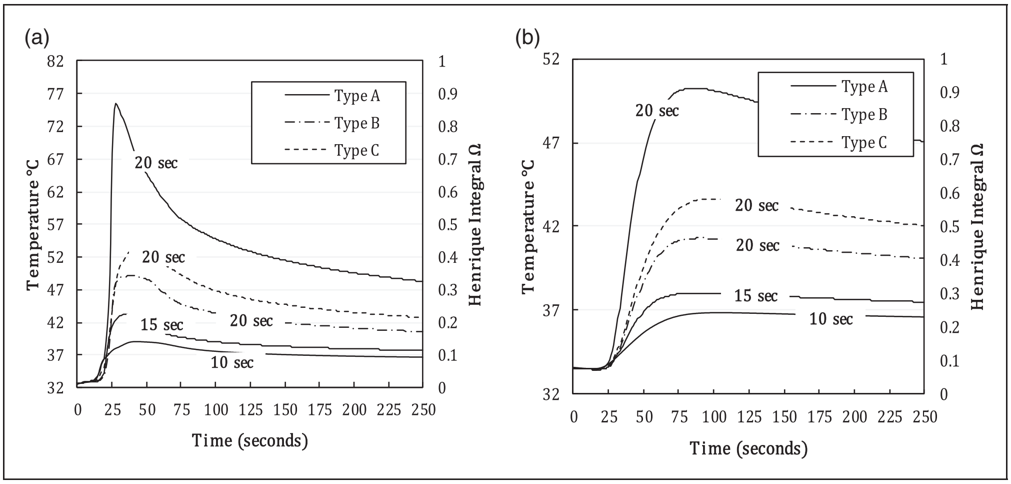

Figure 10. Predicted skin temperature at an incident flux of 126 kW/m^2. (a) Basel layer and (b) dermal base.

layer, type B retained skin temperature 36% below the type A maximum estimated temperature, and type C at 31% as compared with type A. At the dermal base, type B performed 18% better and type C performed 14% better. These percentages signify a reduction in skin temperature.

Discussion

The significance of auxiliary layers is estimated based on superficial burn injuries. Type B and type C provided more protection by delaying the time to burn injuries. In the case of type A, no burn is predicted for an incident heat flux of 84 kW/m^2 and 126 kW/m^2 under exposure durations of 20 and 15 s, respectively. For type A exposed to 84 kW/m^2 for 25 s a first-degree burn is estimated at 35 s, and a second-degree burns at 37th second. This close gap is associated with a rapid increase in skin temperature due to OS failure as evident from Figure 10. Similarly, type A exposed to 126 kW/m^2 for 20 s; a 2nd – degree burn is projected at 24 s, and a third-degree burn at 74 s. In the case of type B, no burn injuries are observed at 84 kW/m^2. At an incident flux of 126 kW/m^2 for 20 s, a first-degree burn is predicted at 35 s. Type C underperformed more than type B with a first-degree burn occurring after 55 s exposed to 84 kW/m^2 for 25 s and a second-degree burn at 30 s exposed to 126 kW/m^2 for 20 s. This comparison is summarized in Table 5.

At life-threatening conditions of 126 kW/m^2 it is shown that a second-degree burn will ensue rapidly after a first-degree burn if OS fabric undergoes thermal degradation. As the Henrique integral is a chemical rate process, it is possible that underlying tissue in the basal layer does not have enough time to react to drastic temperature variations. As a result, skin tissues undergo chemical changes rapidly causing a second-degree burn. The auxiliary protective layers are therefore recommended for firefighters involved in severe fire conditions.

Table 5. Time to superficial burn Injury

Incident flux [q_{inc}] kW/m^2	Exposure time (s)	Burn Injuries (s)		
		First	Second	Third
Type A				
84	10	no	no	no
	20	no	no	no
	25	35	37	no
126	10	no	no	no
	15	no	no	no
	20	–	24	74
Type B				
84	10	no	no	no
	20	no	no	no
	25	no	no	no
126	10	no	no	no
	15	no	no	no
	20	35	no	no
Type C				
84	10	no	no	no
	20	no	no	no
	25	55	no	no
126	10	no	no	no
	15	no	no	no
	20	–	30	no

In vertical orientation garment assembly performs well by protecting for a prolonged duration of time.[60] For type A lay-up, burn injuries predicted by a similar experimental study of Mandal and colleagues[61] in a horizontally configured apparatus showed that under exposure of 84 kW/m^2, a second-degree burn occurs after 20.6 s and under radiant exposure of 50 kW/m^2

after 28.7 s. It is evident that orientation dependence on burn prediction is dominant. This behavior of prolonged burn injury time has also been documented in vertically orientated tests conducted by Udayraj and Wang,[10] concluding that for a single-layered protective garment transmitted thermal energy in the bench-scale test is dependent on test configuration, and horizontally oriented test apparatus underestimates the protective performance of the garment. This behavior was also confirmed for multilayer garments in another study by Mandal and colleagues.[2] The authors also reached the same conclusion as Udayraj and Wang,[10] when they compared bench-scale test (horizontal orientation) results with their vertical scale apparatus (hexagonal shaped). The results, obtained from this study, complement the recent trends in the industry and provide knowledge on the performance of outer garment suits at life-threatening fire conditions beyond previous through the limit of 84 kW/m^2. The results also encourage the utilization of vertical bench-scale apparatus for all types of exposures, which can be an alternative/reliable set-up to the existing established horizontal bench-scale tests recommended by international standards such as ISO,[17] NFPA[16] or ASTM.[62]

Skin temperature profile

The burn injuries can occur due to: (a) fabric layers failure under exposure; (b) stored thermal energy in the fabric layers; and (c) prolonged exposure duration. To understand this, the temperature profile for three skin layers: epidermis, dermis, and subcutaneous are studied further. In Figure 11 and Figure 12, temperature profiles of the skin layer representative of four distinct phases of the experiment are shown. Three temperature points defining one temperature profile are plotted as: (a) the first point represents the epidermis surface temperature; (b) the second point represents the basal layer temperature; and (c) the last point represents dermal base temperature.

Skin temperature profile at an incident flux of 84 kW/m^2 for 25 s exposure time is plotted in Figure 11, for type A (conventional lay-up), type B (enhanced lay-up using Nomex underlayer) and type C (enhanced lay-up using honeycomb structure layer). The temporal significance of each line is as follows:

a. $t = 0$ s, representative of skin temperature distribution before thermal load.
b. $t = 15$ s, skin temperature distribution mid-way into an experiment.
c. $t = 25$ s, when the thermal load is removed.
d. $t = 50$ s, maximum skin temperature representing the effect of stored thermal energy in fabric.

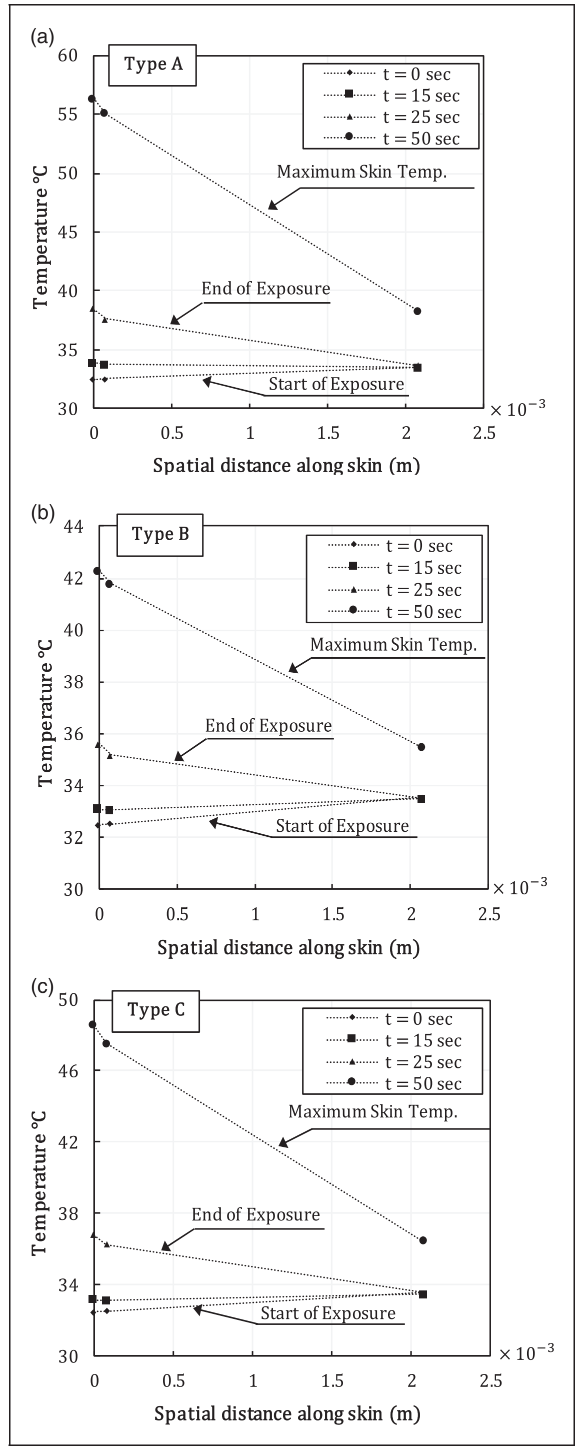

Figure 11. Predicted skin temperature profile at an incident flux of 84 kW/m^2 for 25 s. (a) Conventional garment layup; (b) (b) enhanced garment layup with underwear and (c) enhanced garment layup with honeycomb.

In all three types of lay-up, a common trend is observed, the skin temperature for the duration of exposure remains within $\Delta T \approx 5°C$. However, it keeps on rising even after the thermal load is removed. This is

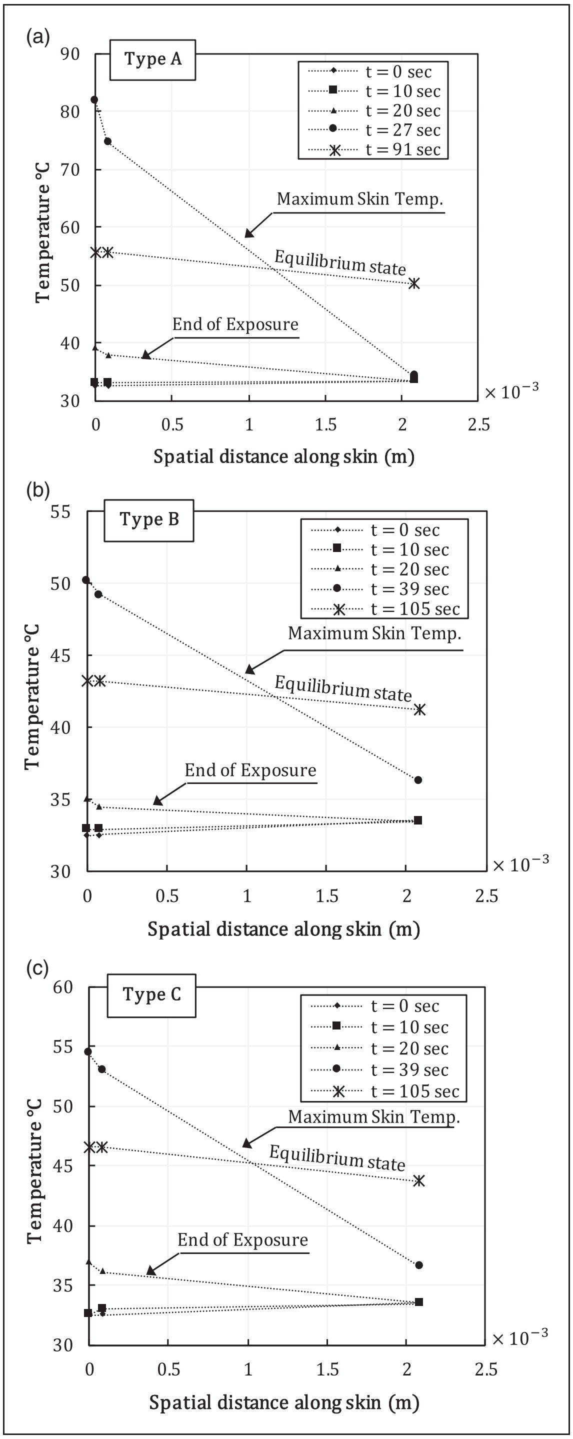

Figure 12. Skin temperature profile at an incident flux of 126 kW/m^2 for 20 s. (a) Conventional garment layup; (b) enhanced garment layup with underwear and (c) enhanced garment layup with honeycomb.

an eminent behavior, which has been reported in past literature,[63–65] but has not been addressed practically. The application of extra underlayers (type B and type C) minimizes this effect. Type B and type C lay-ups showed significant improvement in mitigating the effects of stored thermal energy. The epidermis surface temperature for type A is predicted to be ≈56°C, reduced in type B to ≈42°C and in type C to ≈49°C. The study of skin layer temperature profiles showed that the temperature slope $\left[\frac{dT}{dx}\right]$ is dependent on the skin layer thickness and the fact that $\frac{dT}{dx}_{epi} < \frac{dT}{dx}_{dermis}$ suggests that the dermis layer due to its thicker structure mitigates thermal energy flow better than the epidermis surface.

In the case of 126 kW/m^2 and an exposure time of 20 s, Figure 12 represents its effect on skin layer temperature distribution. The time to reach maximum temperature varies with the lay-up. For type A, the skin tissue temperature reaches its maximum value after 27 s. For type B and type C, this is increased to 39 s. All burn injuries occur during the cool down period. In the case of 126 kW/m^2, even though type B and type C limited epidermis surface temperature by ≈38–32%, as compared with type A, it still exceeds the threshold level of pain. Nevertheless, the time to reach maximum skin temperature is improved by 12 s. The dermal base temperature remains close to the average core body temperature of ≈37°C, even when the epidermis surface temperature reaches its highest value. This high surface temperature starts dropping with an increase in the core body temperature until it reaches its equilibrium state. The protective lay-up of type B and type C kept this equilibrium state below or close to the threshold level with type B being the most effective by maintaining it at 44°C.

Implications on thermal comfort and moisture

Adding an extra layer to the existing protective suit has proved to mitigate burn injuries. However, the implications of the thermal comfort of firefighters with added layers is not addressed in this study. Application of the honeycomb structure between the MB and the TL is demonstrated to be beneficial. Due to the difficulties in retaining its shape during an active routine, it is advised to insert it at the front chest or back area. Consequently, it is not recommended, as it will restrict mobility. In comparison, the meta-aramid fabric layer is comfortable and can easily be worn inside an existing suit. More work needs to be done to assess the thermal comfort of auxiliary layers. Based on current work, type B lay-up is recommended. However, care must be taken while implementing the results of this study to real-life conditions as the assessment is done under laboratory conditions. Furthermore, the results of the current study are limited to dry garments only and future studies are required for moisture transport and the effect of physical changes for the four-layered garment.

Conclusions

Three types of protective suit lay-ups were tested: type A (convectional lay-up); type B (added layer of meta-aramid fabric); and type C (added extra layer of a honeycomb structure made of Nomex). Their performance level is accessed under extreme conditions of 84 kW/m^2 and life treating condition of 126 kW/m^2. For type A, a second-degree burn is predicted after 37 s when exposed to 84 kW/m^2 for 25 s, and a second-degree and third-degree burn after 24 s and 74 s when exposed to 126 kW/m^2 for 20 s. The temperature at the epidermis layer remained lower than the threshold level of 44°C for the incident flux of 84 kW/m^2. Only a first-degree burn is predicted for the incident flux of 126 kW/m^2 for an exposure time of 20 s. For type C, a first-degree burn is predicted after 55 s under 84 kW/m^2 and a second-degree burn after 30 s under 126 kW/m^2. The key highlights of the study are: (a) All burn injuries are due to stored thermal energy and occurred after exposure has ended. This impact is reduced with the proposed auxiliary layer of meta-aramid fabric, between the TL and skin, at a distance 5 mm away from the TL and 2 mm behind the skin. (b) The implementation of meta-aramid as an auxiliary layer mitigated second and third-degree burn injuries. (c) The addition of a meta-aramid fabric layer proved to be more beneficial in delaying time to burn injuries compared with conventional lay-up or honeycomb structure layer. The honeycomb structure layer is not recommended as it restricts user mobility.

Acknowledgements

The authors express our gratitude to Dr. Sungwook Kang and Dr. J. Yoon Choi at Korean Conformity Laboratories (KCL) in South Korea for their support in procurement of the test materials and for providing technical assistance during the experiments.

Declaration of conflicting interests

The author(s) declared no potential conflicts of interest with respect to the research, authorship, and/or publication of this article.

Funding

The author(s) disclosed receipt of the following financial support for the research, authorship and/or publication of this article: This project is funded by National Fire Agency through R&D programme on Development of Fire Safety Technologies for Emergency Response to Fire Hazards (Grant No. 20008021).

ORCID iDs

Rumeel A Bhutta https://orcid.org/0000-0002-4745-0493
Sengkwan Choi https://orcid.org/0000-0001-6427-9897

References

1. Song G, Mandal S and Rossi RM. *Thermal protective clothing for firefighters*. WoodHead Publishing, 2016. DOI: 10.1016/B978-0-08-101285-7.09994-9
2. Mandal S, Annaheim S, Pitts T, et al. Studies of the thermal protective performance of fabrics under fire exposure: from small-scale to hexagon tests. *Text Res J* 2018; 88: 2339–2352.
3. Abbott NJ and Schulman S. Protection from fire: nonflammable fabrics and coatings. *J Coat Fabr* 1976; 6: 48–64.
4. Rossi R. Fire fighting and its influence on the body. *Ergonomics* 2003; 46: 1017–1033.
5. Udayraj, Talukdar P, Das A, et al. Estimation of radiative properties of thermal protective clothing. *Appl Therm Eng* 2016; 100: 788–797.
6. Ghazy A and Bergstrom DJ. Numerical simulation of transient heat transfer in a protective clothing system during a flash fire exposure. *Numer Heat Transf Part A Appl* 2010; 58: 702–724.
7. lu Y, Song G, li J, et al. The impact of air gap on thermal performance of protective clothing against hot water spray. *Text Res J* 2015; 85: 709–721.
8. Sun G, Yoo HS, Zhang XS, et al. Radiant protective and transport properties of fabrics used by wildland firefighters. *Text Res J* 2000; 70: 567–573.
9. Rezazadeh M and Torvi DA. Assessment of factors affecting the continuing performance of firefighters' protective clothing: a literature review. *Fire Technol* 2011; 47: 565–599.
10. Udayraj and Wang F. A three-dimensional conjugate heat transfer model for thermal protective clothing. *Int J Therm Sci* 2018; 130: 28–46.
11. Tsai KC. Orientation effect on cone calorimeter test results to assess fire hazard of materials. *J Hazard Mater* 2009; 172: 763–772.
12. Su Y, Li R, Yang J, et al. Developing a test device to analyze heat transfer through firefighter protective clothing. *Int J Therm Sci* 2019; 138: 1–11.
13. Lawson JR and Twilley WH. *Development of an apparatus for measuring the thermal performance of fire fighters' protective clothing*. U.S. Dept. of Commerce, Technology Administration, National Institute of Standards and Technology. See http://agris.fao.org/agris-search/search.do?recordID=US201300105246 (1999, accessed 6 May 2019).
14. Shaid A, Wang L, Padhye R, et al. Low cost bench scale apparatus for measuring the thermal resistance of multi-layered textile fabric against radiative and contact heat transfer. *HardwareX* 2019; 5: e00060.
15. Behnke WP. Predicting flash fire protection of clothing from laboratory tests using second-degree burn to rate performance. *Fire Mater* 1984; 8: 57–63.
16. NFPA: 1971. *Standard on Protective Ensembles for Structural Fire Fighting and Proximity Fire*

Fighting. Quincy, MA: National Fire Protection Association, 2018.
17. BSI. BS EN ISO: 6942. *Protective clothing – Protection against heat and fire – Method of test: Evaluation of materials and material assemblies when exposed to a source of radiant heat*. London, UK: BSI Standard Publications, 2015.
18. Lawson J. Fire fighters' protective clothing and thermal environments of structural fire fighting. In: *Performance of Protective Clothing: 6th vol*. PA 19428-2959. West Conshohocken: ASTM International, 1997, pp. 334–319.
19. Bwalya A, Gibbs E, Lougheed G, et al. Heat release rates of modern residential furnishings during combustion in a room calorimeter. *Fire Mater* 2015; 39: 685–716.
20. Song G, Ding D and Chitrphiromsri P. Numerical simulations of heat and moisture transport in thermal protective clothing under flash fire conditions. *Int J Occup Saf Ergon* 2008; 14: 89–106.
21. Sawcyn CMJ and Torvi DA. Improving heat transfer models of air gaps in bench top tests of thermal protective fabrics. *Text Res J* 2009; 79: 632–644.
22. Torvi DA and Threlfall TG. Heat transfer model of flame resistant fabrics during cooling after exposure to fire. *Fire Technol* 2006; 42: 27–48.
23. Congalton D. Shape memory alloys for use in thermally activated clothing, protection against flame and heat. *Fire Mater* 1999; 23: 223–226.
24. Torvi DA and Dale JD. Effects of variations in thermal properties on the performance of flame resistant fabrics for flash fires. *Text Res J* 1998; 68: 787–796.
25. Hao L and Yu W. Comparison of thermal protective performance of aluminized fabrics of basalt fiber and glass fiber. *Fire Mater* 2011; 35: 553–560.
26. Jin L, Park PK, Hong KA, et al. Effect of aluminized fabrics on radiant protective performance of fire proximity suit materials. *Ann Occup Hyg* 2014; 59: 243–252.
27. Naeem J, Mazari A, Volesky L, et al. Effect of nano silver coating on thermal protective performance of firefighter protective clothing. *J Text Inst* 2019; 110: 847–858.
28. Li X, Wang Y and Lu Y. Effects of body postures on clothing air gap in protective clothing. *J Fiber Bioeng Informatics* 2011; 4: 277–283.
29. Psikuta A, Frackiewicz-Kaczmarek J, Frydrych I, et al. Quantitative evaluation of air gap thickness and contact area between body and garment. *Text Res J* 2012; 82: 1405–1413.
30. Jin L, Yoon KJ, Hong K, et al. Effect of aerogel on thermal protective performance of fire-fighter clothing. *J Fiber Bioeng Informatics* 2013; 6: 315–324.
31. Qi Z, Huang D, He S, et al. Thermal protective performance of aerogel embedded firefighter's protective clothing. *J Eng Fiber Fabr* 2013; 8: 155892501300800.
32. Mercer GN and Sidhu HS. A theoretical investigation into phase change clothing benefits for firefighters under extreme conditions. *Chem Prod Process Model*; 4. Epub ahead of print 30 January 2009. DOI: 10.2202/1934-2659.1349
33. Phelps H and Sidhu H. A mathematical model for heat transfer in fire fighting suits containing phase change materials. *Fire Safety J* 2015; 74: 43–47.
34. Rossi RM and Bolli WP. Phase change materials for the improvement of heat protection. *Adv Eng Mater* 2005; 7: 368–373.
35. Zhu FL, Feng QQ, Liu R, et al. Enhancing the thermal protective performance of firefighters' protective fabrics by incorporating phase change materials. *Fibres Text East Eur* 2015; 2: 68–73.
36. Hu Y, Huang D, Qi Z, et al. Modeling thermal insulation of firefighting protective clothing embedded with phase change material. *Heat Mass Transf* 2013; 49: 567–573.
37. Shaid A, Wang L, Fergusson SM, et al. Effect of aerogel incorporation in PCM-containing thermal liner of firefighting garment. *Cloth Text Res J* 2018; 36: 151–164.
38. Eryuruk SH, Koncar V, Kalaoglu F, et al. Thermal comfort properties of firefighters' clothing with underwear. *IOP Conf Ser Mater Sci Eng* 2018; 459: 012040.
39. Du F and Li X. The approach of honeycomb sandwich structure for thermal protective clothing. *J Ind Text* 2021; 50(7): 957–969.
40. Kang S, Kwon M, Choi JY, et al. Development of Testing Environment for Thermal Protective Clothing at Critical Conditions. In: *The Proceedings of 11th Asia-Oceania Symposium on Fire Science and Technology*. Singapore: Springer Singapore, pp. 435–449.
41. Mell WE and Lawson JR. A heat transfer model for firefighters' protective clothing. *Fire Technol* 2000; 36: 39–68.
42. Song G. *Modeling Thermal Protection Outfits for Fire Exposures*. PhD Thesis, North Carolina State University. See https://repod.lib.ncsu.edu/handle/1840.16/5766 (2003, accessed 6 May 2019).
43. Song G. Cothing air gap layers and thermal protective performance in single layer garment. *J Ind Text* 2007; 36: 193–205.
44. GUARD RW-3 – Underwear – CLOTHING – racing | Sparco Official. See https://www.sparco-official.com/en/racing/clothing/underwear/guard-rw-3-22593.html (2019, accessed 9 May 2019).
45. Aramid paper honeycomb core-Jiaxing CMAG Composite Material Co., Ltd. See http://www.cmag.com.cn/en/product/html/?152.html (accessed 9 May 2019).
46. Henriques FC Jr and Moritz AR. Studies of thermal injury: i. the conduction of heat to and through skin and the temperatures attained therein. A theoretical and an experimental investigation. *Am J Pathol* 1947; 23: 530.
47. Henriques FC. Studies of thermal injury; the predictability and the significance of thermally induced rate processes leading to irreversible epidermal injury. *Arch Pathol* 1947; 43: 489–502.
48. Stoll AM and Chianta MA. *A Method and Rating System for Evaluation of Thermal Protection*. See https://apps.dtic.mil/docs/citations/AD0846419 (1968, accessed 6 May 2019).
49. Stoll AM and Greene LC. Relationship between pain and tissue damage due to thermal radiation. *J Appl Physiol* 1959; 14: 373–382.

50. Pennes HH. Analysis of tissue and arterial blood temperatures in the resting human forearm. *J Appl Physiol* 1948; 1: 93–122.
51. Torvi DA and Dale JD. A finite element model of skin subjected to a flash fire. *J Biomech Eng* 1994; 116: 250.
52. Lipkin M and Hardy JD. Measurement of some thermal properties of human tissues. *J Appl Physiol* 1954; 7: 212–217.
53. Logan DL. *A first course in the finite element method*. Boston, Massachusetts: Cengage Learning, 2012.
54. Ozisik N, Orlande HRB, Colaço MJ, et al. *Finite Difference Methods in Heat Transfer,* 2nd ed. Boca Raton: Chapman and Hall/CRC, 2017.
55. Griffith MV and Horton GK. The transient flow of heat through a two-layer wall. *Proc Phys Soc* 1946; 58: 481–487.
56. Stoll AM, Chianta MA and Munroe LR. Flame-contact studies. *J Heat Transfer* 1964; 86: 449.
57. Weaver JA and Stoll AM. *Mathematical model of skin exposed to thermal radiation*. Naval air development center, Warminster. See https://apps.dtic.mil/docs/citations/AD0659973 (1967, accessed 17 May 2019).
58. ISO. ISO:13506-1. Protective clothing against heat and flame – Test method for complete garments – Prediction of burn injury using an instrumented manikin. London: BSI Standard Publication, 2017. 3.
59. Gaussian Models – MATLAB and Simulink – MathWorks United Kingdom. See https://uk.mathworks.com/help/curvefit/gaussian.html (2019, accessed 31 May 2019).
60. Bhutta RA and Sengkwan C. Thermo-physical evaluation of firefighter outer garment in high flux environments. *Text Res J* 2022; 92: 00405175221086043.
61. Mandal S, Song G, Ackerman M, et al. Characterization of textile fabrics under various thermal exposures. *Text Res J* 2013; 83: 1005–1019.
62. ASTM international. ASTMF2703-08. Standard Test Method for Unsteady – State Heat Transfer Evaluation of Flame Resistant Materials for Clothing with Burn Injury Prediction. West Conshohocken, PA: ASTM International.
63. Song G, Cao W and Gholamreza F. Analyzing stored thermal energy and thermal protective performance of clothing. *Text Res J* 2011; 81: 1124–1138.
64. He J and Li J. Analyzing the transmitted and stored energy through multilayer protective fabric systems with various heat exposure time. *Text Res J* 2016; 86: 235–244.
65. Barker R, Guerth C, Behnke W, et al. Measuring the thermal energy stored in firefighter protective clothing. In: Nelson C, Henry N (eds) *Performance of Protective Clothing: Issues and Priorities for the 21st Century: Seventh Volume*. West Conshohocken, PA: ASTM International, pp. 33–44.